Carpathian Journal of Earth and Environmental Sciences, August 2018, Vol. 13, No. 2, p. 343 - 358; DOI:10.26471/cjees/2018/013/030

MICROMORPHOLOGICAL ASPECTS OF FLOODED SOILS IN MASOULE RUDKHAN WATERSHED, NORTH OF IRAN

Mehdi NOROUZI [1*], Ali Asghar JAFARZADEH [1], Hassan RAMEZANPOUR [2], Farzin SHAHBAZI [1] & Mohammadreza KHALEDIAN[3,4]

[1]*Department of Soil Science, Faculty of Agriculture, University of Tabriz, Iran*
[2]*Department of Soil Science, Faculty of Agriculture, University of Guilan, Rasht, Iran*
[3]*Water Engineering Department, Faculty of Agricultural Sciences, University of Guilan, Rasht, Iran*
[4]*Department of Water Engineering and Environment, Caspian Sea Basin Research Center, Rasht, Iran.*
[*]*Correspondence author; E-mail: Mehdi_uni2000@yahoo.com*

Abstract: Flooding leads to many problems which are the major concerns of environment and society in north of Iran. Therefore, our knowledge increasing about flooding and identification of its source could be useful to decline devastating effects of floods. This study was conducted to investigate the micromorphological aspects of flooded soils in Masoule Rudkhan watershed, north of Iran. Four soil pedons were selected in representative (non-flooded) soil (P1) and flooded soil (P2) in the upstream with shale parent rock and representative soil (P3) and flooded soil (P4) in downstream with greenschist parent rock, respectively. Soil profile description and sampling were carried out based on soil survey manual and after analyzing of samples, soils were classified as Typic Udifluvents in the flooded soils, Typic Dystrudepts and Typic Hapludualfs in representative soil developed on shale and greenschist parent rocks, respectively. Based on obtained results there are lithologic discontinuities in flooded soils that can be confirmed by micromorphology observations. This soils microstructure ranges from a massive to weakly developed granular and weak developed sub-angular blocky and vughs were prominent. Although chitonic c/f-related distribution was the most common in the representative soils, but the prominent one was porphyric. The fine fraction mainly had stipple and mosaic speckled b-fabric, while stipple speckled and crystallitic b-fabrics observed in flooded soils. No signs of clay illuviation were observed in flooded soils, while flood coating and lignin-rich plant residues, rock fragments, charcoal, artefacts and so different mineral fragments were most widespread. Presence of calcite features as nodule and coatings, as well as pyroxene and olivine minerals were remarkable in flooded soils that have been derived by calcareous rocks, local bedrocks (gabbro and peridotite), the reworking of deposits and aggregates. The calculated micromorphological index of soil evolution (MISECA) revealed weakly developed Udifluvents in the flooded soils. Generally, soils and susceptibility of parent rock could be as key factors for source routing of flooding, that some micromorphological aspects and mineral identification could be powerful tools for this target.

Keywords: Charcoal, Clay coating, Micritic, MISECA index, Pedorelicts, Pyroxene

1. INTRODUCTION

Floods are considered as the most catastrophic natural disasters and affect an estimated 520 million people across the world yearly, resulting up to 25,000 annual deaths (Teegavarapu, 2012).

In the lands under severe floods, the cracks are filled with coarse sand and gravels (Achyuthan & Fedoroff, 2008). The micromorphological observations of Angelucci (2006) in Alentejo region, Portugal showed that the sedimentary matrix was formed from cyclical flooding. These sediments include: quartz, feldspars grains, minor quantities of micas, hornblende, and the occasional presence of rock fragments such as granite, quartzite and gneiss. Courty et al., (2008) reported that environmental disturbance was specified by sharp depositional contact over the structureless fine sand which resulting from extensive flooding. In Ubeidiya, Mallol (2006) recorded the sand-sized elements relatively rounded in the gravelly layers of floodplain. These layers were overlain by cobble-rich sediments or cobble beds with massive to weakly angular blocky microstructure. Moreover, few plane and channels voids were occurred within undifferentiated b-fabric. Zhuang et al., (2013) with study of floodplain of Yuezhuang site (China) reported that weakly developed soils are characterized by the formation of thin dusty clay coatings, indicating high groundwater levels and relatively poor drainage. During irrigation or flooding, when the floodwaters contain suspended materials, they may flow down and become deposited to form whole-soil coatings at various depths (Fitzpatrick, 1984). In East Pakistan, flood coatings have been observed in seasonally flooded soils. They were weakly oriented coarse clay and silt covering the larger conducting pores in flooded soils (Brammer, 1971). These coatings form very rapidly (within 1 to 2 years) and could be quickly destroyed. They differ from clay coating (argillans) not only in the speed of development, but also in their composition (Brammer, 1971).

Khormali et al., (2003) represented micromorphological index for soil evolution (MISECA) in highly calcareous arid to semiarid conditions. This index also showed good correlation with soil evolution in humid and subhumid regions (Ghergherechi et al., 2009). In this index, several micromorphological parameters such as microstructure, b-fabric, clay coatings, decalcified zone, Fe/Mn oxide and degree of alteration of mineral grains were rated for degree of soil development. The MISECA values theoretically ranged from 0 (non-developed) to 24 (well-developed). Eze et al., (2016) reported that MISECA as a micromorphological index for soil development was suitable for flooded soils.

Masoule Rudkhan watershed in the north of Iran is potentially important area for geology and geomorphology studies. This area is located in Alborz zone, and influenced by tectonic movements, flooding and mass flow. Recent severe flood events in this watershed have raised public awareness for its impacts on environment. However, the identification of the flooding effects on soil properties and micromorphological aspects can be revealed new facts about floods and their origins. The objective of research work was focusing on the investigation of micromorphological aspects of flooded soils in two different parent rocks of Masoule Rudkhan watershed.

2. MATERIAL AND METHOD

2.1. Field Description

This research work was carried out in Masoule Rudkhan watershed of Guilan province, which is located in rainy forest and dense topography, between 37° 6′ to 37° 12′ north latitude and 48° 55′ to 49° 10′ east longitude (Fig. 1). Mean slope and altitude of watershed were 43% and 1436 m from above sea level, respectively. It is considerable that topography causes variations in the genesis and depth of soils. Mean annual precipitation at the nearest meteorological station (Masoule synoptic station) is 1359 mm (1961-2010), without any dry season. Mean annual temperature is 16°C and average annual relative humidity is 81.3%, with high relative humidity of 94% especially in the summer. Soil moisture and temperature regimes are udic and mesic, respectively (Soil and water research institute, 1998). The vegetation of watershed is deciduous forest dominated by Carpinus betelus, Fagus orientalis, Zelkova carpinifolia, Acer insigne, Mespilus germanica, and Alnus subcordata (Nael et al., 2013).

2.2. Geology

The study area is completely known from geological aspect and very diverse and dominated by Precambrian and Paleozoic metamorphic and mafic rocks, covered by Jurassic, Cretaceous shale and limestone. The Precambrian and Paleozoic rocks of the area consist of phyllite, quartzite, phyllitic schist, phyllitic slate, marble, diorite, metamorphic tuff, mica schist, gabbro (Darvishzade, 2002), peridotite, pegmatite, greenschist, dolerite (Rezapour et al., 2014) and tonalite (Nael et al., 2013).

2.3. Soil sampling and description

Using API (Application Program Interface) and integrating DEM with GIS, and information from Natural Resources Organization and native people, soil pedons were excavated and then described. Four soil pedons in two parent rocks (greenschist and shale) from foot slope positions of Masoule Rudkhan watershed were selected and sampled. Soil morphological characteristics were described based on the field book for describing and sampling soils (Schoeneberger et al., 2012) and soil survey manual (USDA, 2017).

2.4. Laboratory analysis

For physical and chemical analyses, soil samples were collected from each horizon and air-dried, then passed through a 2 mm (10 mesh) sieve. Soil colour was determined according to Munsell soil colour charts. Hydrometer method was used for determining particle size distribution (Gee & Or, 2002). Soil pH was determined in saturated soil paste (Thomas, 1996). Electrical conductivity (EC) was detected using conductivity meter in a saturation extract of soil (Rhoades, 1996). Equivalent calcium carbonate (CCE) was measured by titration with acid (Loeppert & Suarez, 2002). The Walkley–Black wet oxidation method was applied for estimation of organic carbon (Nelson & Sommers, 1996). Cation exchange capacity (CEC) was determined by saturation with 1M ammonium acetate (NH_4OAc) at pH=7.0 (Sumner & Miller, 1996). Exchangeable cations such as (Ca, Mg, Na and K) were extracted using 1M NH_4OAc (pH=7.0). Na and K concentrations were determined by flame emission spectrometer (Suarez, 1996) and Ca and Mg concentrations were measured by titration with Ethylenediaminetetraacetic acid disodium salt (EDTA disodium) solution (Helmke & Sparks, 1996).

2.5. Micromorphological analyses

For micromorphological study, soil thin sections were prepared from air-dried undisturbed and oriented clods using standard techniques described by Murphy (1986). Micromorphological descriptions were carried out in plane polarised (PPL) and crossed polarised lights (XPL) using a polarizing microscope (ZEISS model) and the definitions based on Bullock et al., (1985) and Stoops (2003). In addition, Micromorphological index of MISECA was measured with rating system presented by Khormali et al., (2003). Area of clay coating and Fe/Mn oxide in this index was measured by image analysis technique (with scale help) in Photoshop software version CC.

3. RESULT

3.1. Genesis and morphological properties

Abbreviated morphological properties of selected pedons were summarized in Table 1 and based on obtained results soils were classified as Typic Udifluvents in the flooded soils, Typic Dystrudepts and Typic Hapludualfs in representative (non-flooded) soil developed on shale and greenschist parent rock, respectively (Soil Survey Staff, 2014). The flooded soil located in upstream (pedon 2) was identified as a buried soil. This soil has been covered with a surface mantle of new soil transported material with 79 cm thick. In this pedon, the C horizons lie directly over CAb horizon. Lithologic discontinuities were observed in the field with 42% gravel in C2 incomparing with 22% gravel in 2CAb of flooded soils. The horizons of the flooded soils had coarse texture comparing to representative soils in both parent rocks. The horizons in most flooded soils exhibit a reddish hue (2.5YR) according to the Munsell color chart, while representative soils had hue of 10YR. The flooded soils in downstream (pedon 4, with greenschist parent rock) were characterized by coarse textured class (sandy, sandy loam and loamy sand). The granular structures were identified in surface horizons of flooded and representative pedons. In the subsurface horizon of representative or control pedons, soil structure was weak to strong subangular blocky. Furthermore, the massive, weak subangular blocky and single grain structures were observed in the subsurface horizon of flooded soils. Therefore, flooded soils were relatively poorly to poorly developed in pedons 2 and 4, respectively. Almost no sign of clay illuviation was observed in flooded soils, while clay coating was observed in the representative or control soils developed on greenschist. The flooded soils showed very slightly and slightly effervescent due to carbonate. The number of gravels in flooded soils were more than representative ones.

3.2. Soil analytical properties

The results of the particle size distribution showed that clay content was higher in representative soils in compared to flooded ones. The highest clay content (mean 340 $g.kg^{-1}$) was found in the horizons of pedon 1 (representative soil developed on shale parent rock) and higher sand contents were found in all the flooded soils. The amount of sand was usually >500 $g.kg^{-1}$ (ranged from 460 to 940 $g.kg^{-1}$) in all the flooded soils, while silt ranged from 70 to 495 $g.kg^{-1}$. Silt was the dominant particle size in representative soil located in downstream with greenschist parent rock. In the sand-sized classes, coarse (0.50–1.00 mm) and very coarse (1.00–2.00 mm) sands were dominant in soils developed on shale parent rock. Unlike, very fine sands (0.05–0.10 mm) and fine sand (0.10– 0.25mm) had the highest content on the soils developed on greenschist. Soil pH was neutral and slighty acidic in representative soil pedon developed on shale parent rock and soil pedon developed on greenschist parent rocks, respectively but the flooded soils had moderately alkaline reaction. EC was extremely low in all the soil pedon and showed no trend with depth. $CaCO_3$ content was lower in horizons of representative soils, and increased in the flooded soils with an average of >34 $g.kg^{-1}$ $CaCO_3$. The greatest amount of $CaCO_3$ was belonged to the flooded soils of downstream and $CaCO_3$ content showed no trend with depth. The soil OC content was higher in the A horizons and showed a downward trend with depth in representative soils, while did not observed the same trend in flooded soils. The exchangeable cations were presented generally in order of abundance Ca > Mg > K > Na. The content of Ca was dominant and above 6.68 cmol+.kg^{-1} in all soils and its content in flooded soils was higher than representative ones. CEC values was generally higher in the A horizons and lower in flooded soils with range of 2.19 to 26.36 cmol+.kg^{-1}, while it ranged from 16.33 to 34.17 Cmol+.kg^{-1} in representative soils. The base saturation (BS) in all horizons was >50% and had not any trend with depth. The BS of flooded soils were high, and was 100% in all horizons in flooded soils in downstream with greenschist parent rock (Table 2).

3.3. Soil micromorphology

3.3.1. Micromorphology of parent rocks

The parent rock in upstream of watershed is shale. It is a sedimentary rock, which typically have a geogenic-laminated structure under pressure and consist predominantly of quartz, heterogeneous feldspar and other opaque minerals. Moreover, chlorite and biotite observed in lower amount (Fig. 2a). The parent rock in downstream was a greenschist with igneous and sedimentary relics (Fig. 2b). This rock is a low-grade metamorphic rock, which retains relics of pre-existing igneous and sedimentary minerals and textures, with metamorphic chlorite, quartz, albite, epidote and primary pyroxene (augite). Furthermore, fragments of shale were abundant in fine-grained matrix of the greenschist rock (Yardley et al., 1990). Calcareous shale, phyllite, gabbro and peridotite were abundant in Masoule Rudkhan watershed. Calcareous shale in study area is in an alteration stage and thinly laminated fine grains. It consists predominantly quartz, mica (muscovite and biotite), chlorite and micritic calcite minerals (Fig. 2c). Micaschist have foliated texture and is characterized by a parallel alignment of muscovite and biotite crystals in a matrix of interlocking quartz crystals (Zauyah et al., 2010) with metal minerals veins (Fig. 2d).

Table 1. Abbreviated morphological properties of horizons for the selected Pedons

Horizon	Depth (cm)	Color (Moist)	Boundary[a]	Texture[b]	Structure[c]	Consistence[d]		Clay film[e]	Effervescence[f]	Gravel (%)
						Moist	wet			
Pedon 1, Representative soil located in upstream (shale parent rock), Fine loamy, Mixed, Superactive, mesic Typic Dystrudept										
Oi	0-2	-	-	-	-	-	-	-	-	
A	2-16	10YR 3/4	cw	cl	2mgr	fr	ss/ps	-	-	20
BAt	16-34	10YR 4/6	gw	cl	1fgr-msbk	fr-fi	ss/ps	-	-	18
Bt1	34-69	10YR 4/4	gs	cl	2msbk	fi	s/p	1mk	-	22
Bt2	69-96	10YR 4/5	gw	cl	2msbk	fi	s/p	-	-	25
C	96-150	10YR 3/6	-	cl	m-1fsbk	fr	ss/ps	-	-	32
Pedon 2, Flooded soil located in upstream (shale parent rock), Fine loamy, Mixed, Superactive, mesic Typic Udifluvent										
Oi	0-1	-	-	-	-	-	-	-	-	-
A	1-13	2.5YR 4/2	cw	scl	2fgr	vfr	ss/ps	-	-	26
AC	13-51	2.5YR 4/3	cw	scl	1fgr-sbk	vfr-fr	ss/ps	-	-	25
C1	51-64	5Y 3/2	cs	sl	m-1fsbk	fr	so/po	-	vs	38
C2	64-79	2.5YR 3/2	as	scl	m	fr	so/po	-	vs	42
2CAb1	79-102	10YR 4/4	gs	scl	m-1fgr	fr-vfr	ss/ps	-	-	22
2CAb2	102-150	10YR 4/3	-	scl	m-1mgr	fr-vfr	ss/ps	-	-	28
Pedon 3, Representative soil located in downstream (greenschist parent rock), Fine loamy, Mixed, Superactive, mesic Typic Hapludalf										
Oi	0-2	-	-	-	-	-	-	-	-	-
A	2-22	10YR 3/4	cw	l	1fgr-fsbk	vfr-fr	ss/ps	-	-	13
Bt1	22-61	10YR 5/7	gs	cl	2msbk	fi	s/p	1mk	-	30
Bt2	61-94	10YR 5/6	cw	sicl	2msbk	fi	s/p	1mk	-	28
BCt	94-119	10YR 3/6	cw	cl	1msbk	fi-fr	s/p	1mk	-	38
CBt	119-150	10YR 4/6	-	l	m-1msbk	fr-fi	ss/ps	-	-	42
Pedon 4, Flooded soil located in downstream (greenschist parent rock), Sandy, Mixed, Superactive, mesic Typic Udifluvent										
Oi	0-1	-	-	-		-	-	-	-	-
A	1-10	2.5YR 3/3	cw	sl	1fgr-m	vfr	ss/ps	-	vs	18
C1	10.26	2.5YR 4/3	cs	ls	sg	vfr	so/po	-	sl	8
C2	26-33	2.5YR 3/2	cs	s	sg	lo	so/po	-	sl	29
2C3	33-39	2.5YR 5/3	cs	sl	m-sg	lo	so/po	-	sl	21
2C4	39-45	2.5YR 4/2	cs	s	sg	lo	so/po	-	sl	40
3C5	45-120	2.5YR 3/1	-	s	sg	lo	so/po	-	sl	76

[a] c = clear, g = gradual; s = smooth, w = wavey; [b] cl= clay loam, l= loamy, ls= loamy sand, sicl= silty clay loam, scl= sandy clay loam, sl= sandy loam, s= sandy; [c] 1 = weak, 2 = moderate; f = fine, m = medium, gr= granular, sbk = subangular blocky, m= massive, sg= single grain; [d] fr = friable, fi = firm, so = nonsticky, ss = slightly sticky, s = moderately sticky, po = nonplastic, ps = slightly plastic, p = plastic; [e]1= few, mk = moderately thick; [f] The gaseous response (seen as bubbles) of soil to applied HCl (carbonate test), vs = very slightly effervescent as few bubbles form, sl = slightly effervescent as numerous bubbles form.

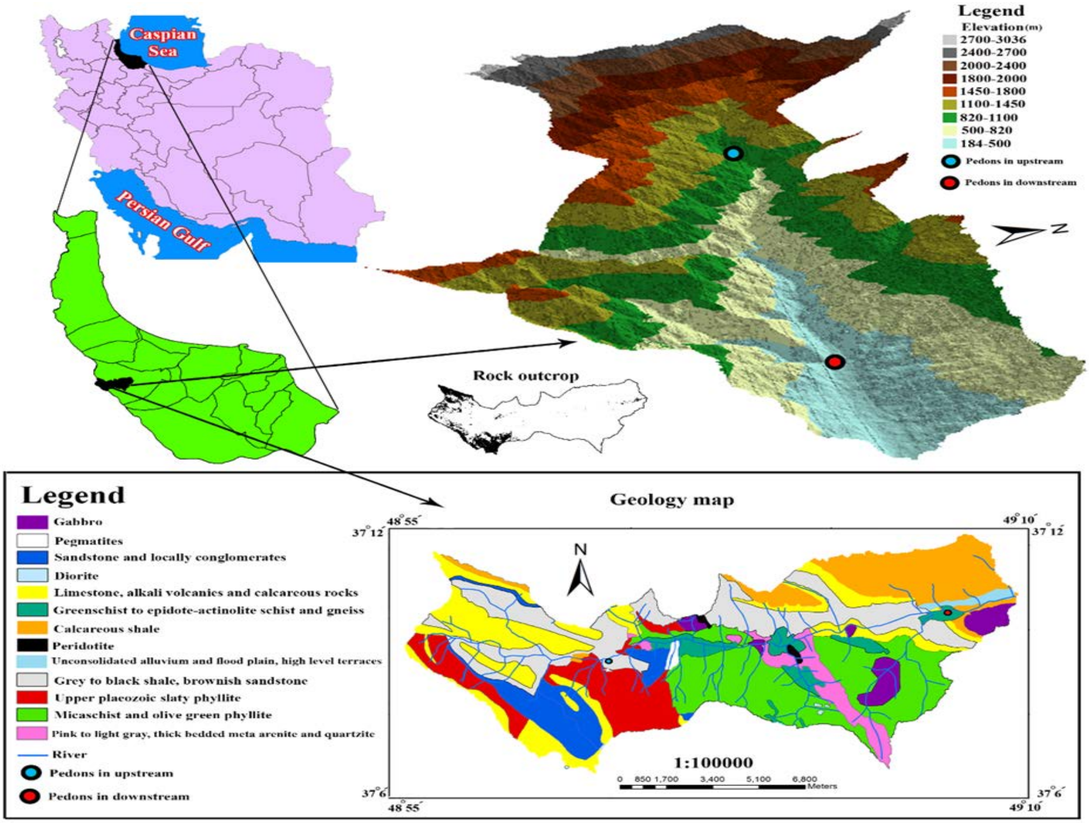

Figure 1. General characteristics of study area

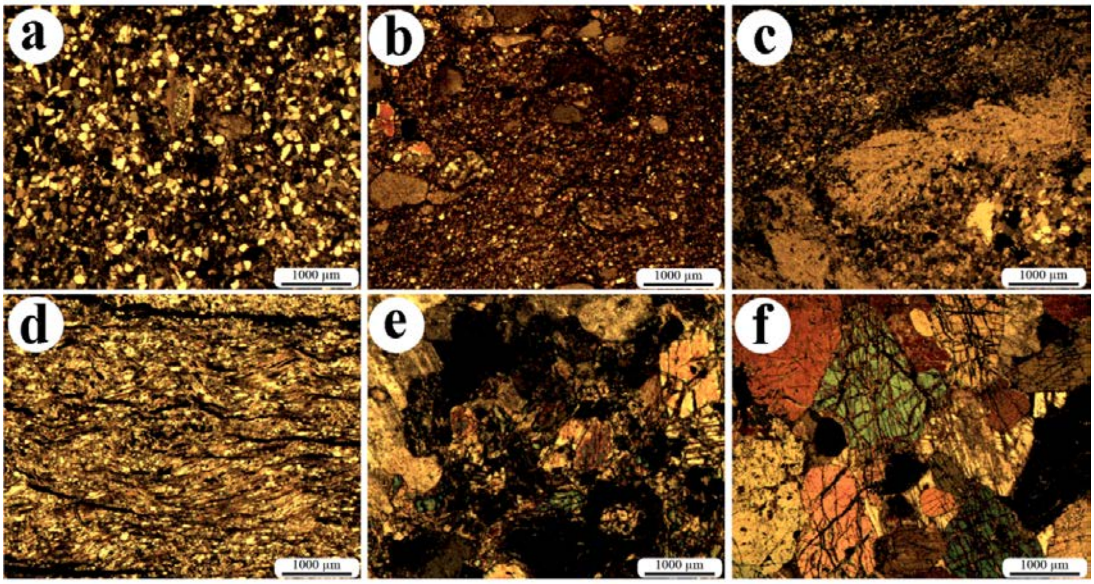

Figure 2. Selected micrographs of thin sections of some parent rocks in watershed, all micrographs are in cross-polarized light (XPL), (a) Shale rock in upstream (Pedons 1 and 2); (b) Greenschist rock in downstream (pedons 3 and 4); (c) Calcareous shale rock; (d) Micaschist rock; (e) Troctolite rock (from gabbroic rocks family) and (f) Wehrlite rock (from peridotite rocks family).

Troctolite is a member of gabbroic rocks family and consists essentially of olivine and plagioclase with varying degrees of sericitic and propylitic alteration and pyroxene (Fig. 2e). The common types of peridotites in the study area was wehrlite, which consists essentially of pyroxene and olivine and low content of plagioclase as inter-cumulus. Most olivines and pyroxenes in wehrlite rock were fresh (Fig 2f). Unlike troctolite, wehrlite rock have not feldspar.

3.3.2. Micromorphology of representative soils

The micromorphological observations of thin sections were detailed in Table 3. The results of soil micromorphological observations generally confirmed field morphological observations. Soil structure in representative pedons (No 1 and 3), was mostly granular, few crumb (Fig. 3a) and subangular blocky (Fig. 3b) in surface and subsurface horizons. Aggregation and faunal activity caused the development of a spongy microstructure in surface horizons (Fig. 3a) and apperaed voids such as vughs, packing (Fig. 3c), channel and chambers (Fig. 3d) in surface and subsurface of Bt horizons. The degree of pedality and ped separation was usually moderate to weak in surface and subsurface horizons, respectively. The main minerals of soils in region were quartz, feldspar and plagioclase usually albite (sodium feldspar) and sometimes anorthite (calcium feldspar) (Fig. 3e). In addition, other minerals such as chlorite (Fig. 3f), muscovite (Fig. 3g), pyroxene (Fig. 3h) and iron opaque grains was identified in thin sections. Weathering of feldspar to sericite was obvious in some horizons (Fig. 3i). Fragments of organ and tissue residues and soil organic matter features was recorded mostly in the surface horizon of representative soils developed in both parent rocks (Fig. 3j). Moreover, the fine fraction in representative soils mainly had stipple and mosaic speckled (Fig. 3k), and locally undifferentiated and grano-striated b-fabrics. Furthermore, unistrial b-fabric rarely observed in some horizons. The prominent c/f-related distribution was open and single to double space porphyric, although chitonic c/f-related distribution patterns were recognized in some horizons. Also, abundant faunal excrements were observed in surface horizon in both representative soils (Fig. 3l). The coarse-fine (c/f) ratio in represented soils was low in compared to flooded soils. The microlaminated clay coatings were recognized in some voids in soils developed on greenschist parent rocks (Fig. 3m). At high magnification, illuvial fragmented clay coatings equivalent to papules (Brewer, 1976) observed in soils developed on shale parent rock (Fig. 3n). Amorphous hypo and quasi coatings of Fe/Mn oxides (Fig. 3o) and the strongly impregnated iron (Fe) and manganese (Mn) oxide nodules with sharp boundaries as typic and geodic nodule were observed (Fig. 3p). The degrees of the soil development calculated by MISECA index ranged from 7 to 13 in representative soils. The maximum values of MISECA index recorded into Bt2 genetic horizons in the representative soil developed on greenschist parent rock located in downstream (Table 3).

3.3.3. Micromorphology of flooded soils

Soil structure was mostly granular in the A and buried horizons (A and CAb). Some weakly developed subangular blocky aggregates observed in subsurface horizons and the degree of pedality was weak to moderate in flooded soils. Soils in downstream (pedon 4) showed single grain to vughy microstructure, the voids of compound packing, planes (Fig. 4a), vugh (Fig 4d), channel and chamber occurred in surface and subsurface horizon, respectively. The microstructure in flooded soils was mainly massive or structureless, although vughs were prominent in soil horizons (Fig. 4b). The textural discontinuities in flooded pedons (No 2 and 4) was observed between horizons (Figs 4a and b). Flooded soils had open and single to double space porphyric and locally chitonic c/f-related distribution pattern (Fig 4c). Various types of b-fabrics such as stipple speckled (Fig. 5c), crystalitic (Fig. 5d) and undifferentiated were recognized which occur in most of the soil horizon and layers. Like representative soils, buried soils in flooded soils of upstream (2CAb2 horizon) showed mosaic speckled b-fabric (Fig. 4d). Furthermore, parts of the parent material have been recognized as unistrial b-fabric (Fig. 4e). The dark colour in A and AC (pedon 2) of flooded soils is mainly caused by finely dispersed organic matter (Fig. 4a). Lignin-rich plant residues (Fig. 4e), organic fine material and organ and tissue residues and decomposed parts were abundant in flooded layers. Moreover, phlobaphene containing bark tissues that was related to acid-producing vegetation such as pine observed in surface horizon (Fig. 4f). The coarse fractions of the soil fabric are dominated by very fine sand-sized quartz, with noticeable contributions of small amounts of irregular shaped, poorly sorted and coarse to very coarse sand-sized minerals. These coarse minerals mainly include quartz, feldspar, muscovite (Fig. 4g), plagioclase (Fig. 5f), pyroxene (Figs. 4h, 5h and p), Olivine (Fig. 5i) and some other opaque minerals. The weathering of biotite to chlorite (Fig. 5g) and weathering of feldspar to resistant minerals such as sericite observed in flooded soils (Fig 4i). A group of calcites features as lighter sparitic and darker micritic calcite nodule and fragments (Figs. 4j, 5j and k) and calcite hypo-coating (Fig. 4k) occurred in both flooded soils. Some irregular calcite showed rhombohedral cleavage (Fig. 5k). The c/f ratio in <10μm soil fraction vary from 50/50 to 95/5. Flooded coating which include mixture of clay, silt and organic matter occasionally were seen in surface horizons (Fig 4m and n). Transported pedofeatures such as the rounded aggregate (Fig 5l), large fresh and irregular rock fragments (Fig. 5m) recorded in flooded soils. The black charcoal fragments were abundant in flooded soils (Figs. 4o and 6o). Faunal excrements (Fig. 5n) and Fe/Mn oxide nodules (Fig. 4p) occasionally found within some soil layers. The calculated MISECA index ranged from 3 to 10 (Table 3).

4. DISCUSSION

Based on obtained results in the flooded soils, microstructure ranged from massive, weak developed subangular blocky to weakly developed granular (Table 3). In flooded soils, the aggregates were poorly formed and partially joined to each other. Gao & Guan (1994) were claimed that under flooded conditions, the glue action of humic material and clay particles did not form aggregates.

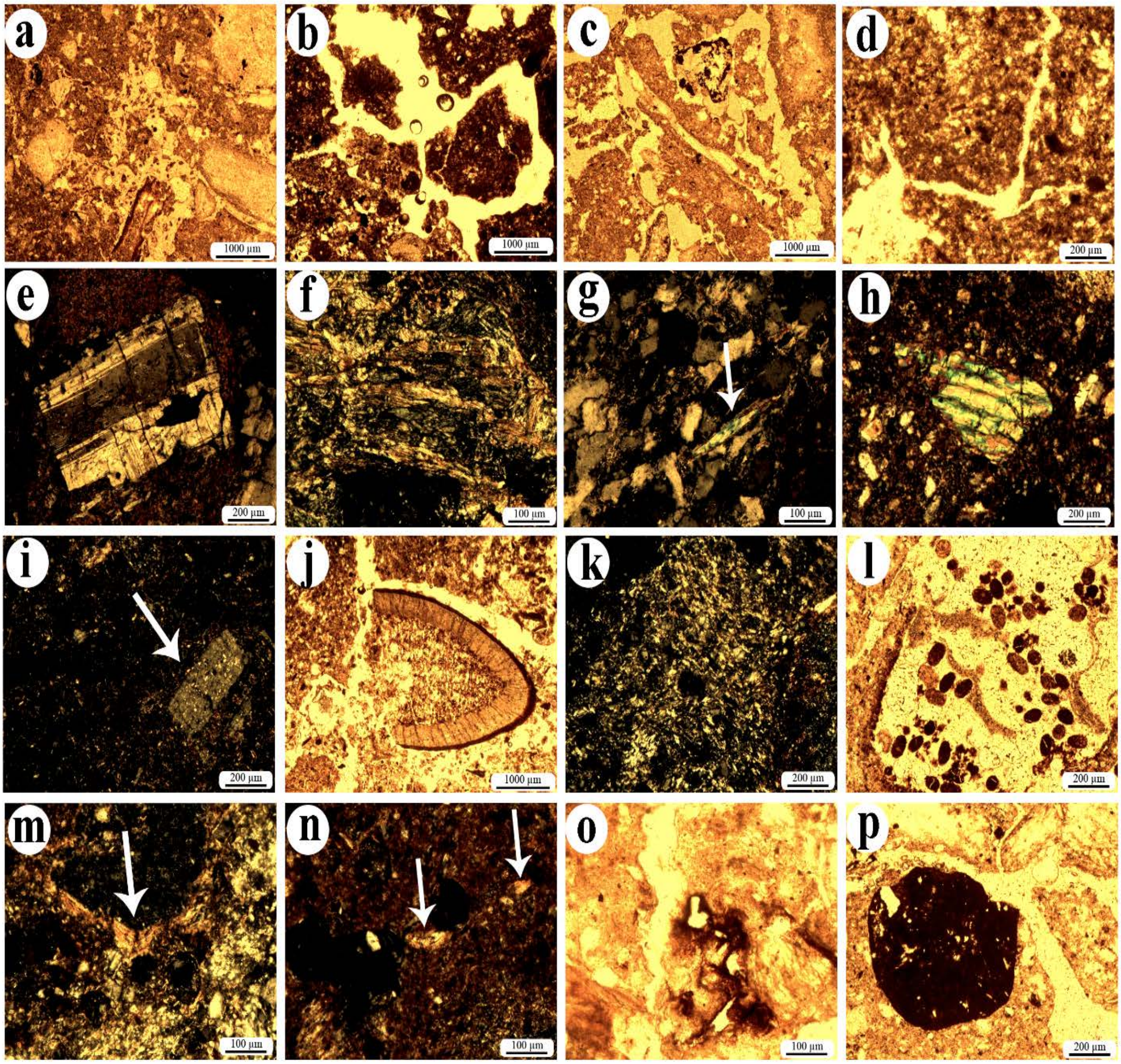

Figure 3. Selected micrographs of thin sections from representative soils developed on shale, pedon 1 (P1) and greenschist, pedon 3 (P3) parent rocks in plain-polarized light (PPL) and cross-polarized light (XPL). (a) Granular aggregate in A horizon of P1, PPL; (b) Subangular blocky aggregate in Bt2 horizon of P3, PPL; (c) Packing void in A horizon of P1, PPL; (d) Channel and chamber voids in Bt1 horizon of P3, PPL; (e) Plagioclase (Anorthite) in Bt1 horizon of P3, XPL; (f) Chlorite mineral in A horizon of P1, XPL; (g) Muscovite mineral in Bt1 horizon of P3 (arrow), XPL; (h) Pyroxene mineral in BCt horizon of P3, XPL; (i) Sericitisation of a feldspar in A horizon of P1(arrow), XPL; (j) Cross sections of the root in A horizon of P3, PPL; (k) Mosaic speckled b-fabric in Bt2 horizon of P3, XPL; (l) faunal excrements which the interior part is consumed by mites in A horizon of P1, PPL; (m) Micro-laminated clay and Fe coatings in Bt2 horizon of P1 (arrow), XPL; (n) Illuvial fragmented clay coatings equivalent to papules in Bt2 horizon (arrows), XPL; (o) Amorphous hypo and quasi coatings of Fe/Mn oxides in C horizon of P3, PPL; (p) Typic Fe/Mn oxide nodule with sharp boundary in BAt horizon of P1, PPL.

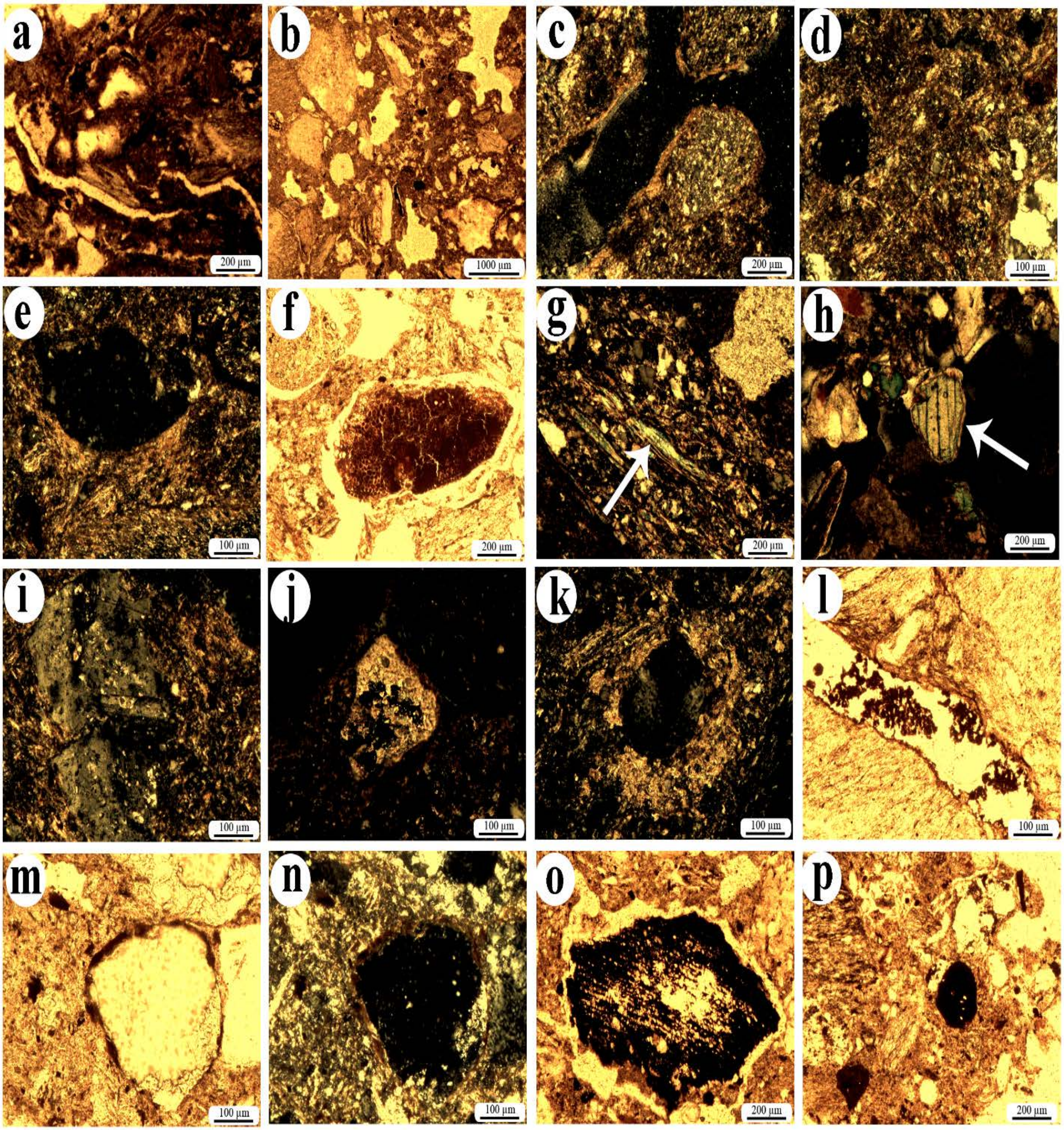

Figure 4. Selected micrographs of thin sections from flooded soils of upstream (Pedon 2), in plain-polarized light (PPL) and cross-polarized light (XPL). (a) Planar void in AC horizon. Dark colour is created by dispersed organic matter, PPL; (b) Vughy structure in AC horizon, PPL; (c) Chitonic c/f-related distribution pattern in C2 horizon, XPL; (d) Mosaic speckled b-fabric and a vugh void (left) in 2CAb2 horizon, XPL; (e) Unistrial b-fabric in C1 horizon, XPL; (f) Phlobaphene containing bark tissues in A horizon, PPL; (g) Muscovite mineral in AC horizon (arrow), XPL; (h) Pyroxene mineral in AC horizon, XPL; (i) Sericitisation of a feldspar in C2 horizon, XPL; (j) An irregular micritic (dark colour), microsparitic and sparitic (light colour) calcite nodule which eroded or dissolved by flow in A horizon, XPL; (k) Calcite hypo-coating in C2 horizon, XPL; (l) Fe/Mn oxide and organic matter hypo-coating on the walls of channel and infilling of organic matter as loose discontinuous in 2CAb2 horizon; PPL; (m) Flooded coating contain mixture of clay, silt and oranic matter in A horizon; (n) Idem in XPL; (o) Charcoal fragment in AC horizon, PPL; (p) Fe/Mn oxide nodules in AC Horizon, PPL.

However, formation of a granular structure in upper horizons of flooded soils could be related to soil fauna. In these soils, the vegetation cover and bioturbation are reflected from some rapidly formed pedological features such as channels, chamber and excrements (Kemp, 2013). Spongy microstructure and excrements incorporation as single and groups of pellets (welded) around organic residual confirm high biological activity in surface horizons of flooded and representative soils. The micromorphological results also indicated a poor action of soil formation processes and aggregation with weathering of some translocated minerals in upper horizons of flooded soils. The c/f-related distribution was porphyric in all soils, with quartz, feldspar and fragments of shale. In the representative soils, weatherable minerals such as plagioclase and biotite were less in surface horizons in compared to subsurface horizon while, there were no regular trend of weathering in flooded soils with sand layers (mostly quartz and feldspar) and light color that have covered by an organic accumulation (dark coloured).

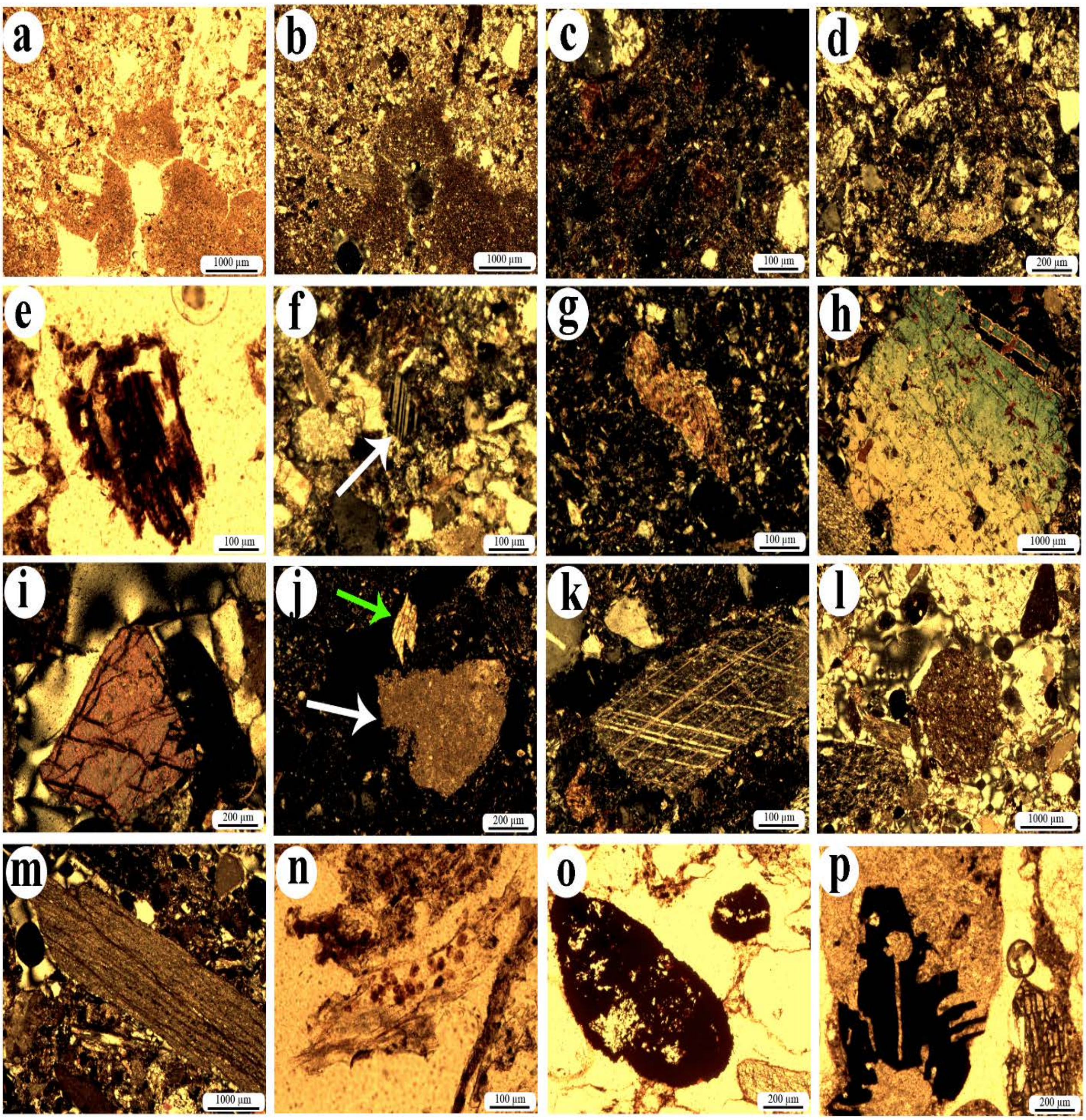

Figure 5. Selected micrographs of thin sections from flooded soils of downstream (Pedon 4), in plain-polarized light (PPL) and cross-polarized light (XPL). (a) Sharp contact between dark soil layer with fine texture and overlying coarse sandy layer (with quartz and feldspar minerals), it shows textural discontinuity between C2 and 2C3 horizons, PPL; (b) Idem in XPL; (c) Stipple speckled b-fabric in C1 horizon, XPL; (d) Calcitic crystallitic b-fabric in C1 horizon, XPL; (e) Lignified tissue in A horizon, PPL; (f) K plagioclase (albite) in C2 horizon, XPL; (g) weathering of biotite to chlorite minerals in 2C3 horizon, XPL; (h) A large weathered pyroxene mineral in 3C5 horizon, XPL; (i) Olivine mineral in 3C5 horizon, XPL; (j) Sparitic (green arrow) and micritic (white arrow) calcite in 2C3 horizon, XPL; (k) Irregular calcite with rhombohedral cleavage in 2C4 horizon, XPL; (l) The aggregate fragment (pedorelict) in 3C5 horizon, XPL; (m) Rock fragment -(lithorelict) of shale in 3C5 horizon, XPL; (n) faunal excrements among the tissue residues in 2C3 horizon, PPL; (o) Charcoal fragments in 3C5 horizon, PPL; (p) A pyroxene mineral (in the right and lower corner) and an artifact piece as iron-based material (left) in 3C5 horizon, PPL.

Table 2. Some physico-chemical properties of horizons for the selected pedons

Horizon	Depth (cm)	Texture ($g.kg^{-1}$)			Sand fraction[1] ($g.kg^{-1}$)					pH[2]	EC[3] ($dS.m^{-1}$)	CCE[4]	OC[5]	Exchangeable cations ($Cmol^{+}.kg^{-1}$)				CEC[6] ($Cmol^{+}.kg^{-1}$)	BS[7] (%)
		Clay	Silt	Sand	VFS	FS	MS	CS	VCS			$g.kg^{-1}$		Na	K	Ca	Mg		
Pedon 1, Representative soil located in upstream (shale parent rock), Fine loamy, Mixed, Superactive, mesic Typic Dystrudept																			
Oi	0-2	-	-	-	-	-	-	-	-	-	-	-	-	-	-	-	-	-	-
A	2-16	345	260	395	48.2	50.4	68.1	120.2	108.1	6.47	0.27	11	46.8	0.24	0.74	11.88	6.76	34.17	57.41
BAt	16-34	335	285	380	45.2	53	66.8	122.5	92.6	6.17	0.08	10	19.5	0.16	0.44	11.14	1.77	29.71	45.44
Bt1	34-69	355	260	385	70.2	46.8	63.8	114.1	90.12	6.26	0.18	12	19.11	0.16	0.34	8.91	9.01	31.42	58.62
Bt2	69-96	350	250	400	74.2	50.1	64.2	122.9	88.75	6.23	0.06	8	14.82	0.24	0.29	9.65	6.84	23.77	71.59
C	96-150	315	240	445	88.9	48.2	66.9	127.3	113.6	6.07	0.07	6	13.26	0.32	0.34	7.17	4.89	16.33	77.89
Pedon 2, Flooded soil located in upstream (shale parent rock), Fine loamy, Mixed, Superactive, mesic Typic Udifluvent																			
Oi	0-1	-	-	-	-	-	-	-	-	-	-	-	-	-	-	-	-	-	-
A	1-13	210	250	540	88.9	77.4	98.1	164.3	111.3	7.37	0.69	22	33.54	0.07	0.34	7.42	6.20	22.36	62.75
AC	13-51	245	235	520	73.8	75.1	98.3	165.2	107.7	7.34	0.74	14	6.24	0.03	0.24	11.88	3.17	16.22	94.48
C1	51-64	195	235	570	77.3	73.4	104	193.1	121.8	7.34	0.29	22	4.68	0.41	0.19	9.65	1.82	14.10	85.59
C2	64-79	220	230	550	80.4	70.6	103	177.4	118.7	7.43	0.63	28	5.46	0.24	0.19	8.17	4.74	14.85	89.82
2CAb1	79-102	275	205	520	71.2	67.7	84.3	176	120.8	7.34	0.33	12	9.36	0.24	0.14	6.68	10.52	20.05	87.71
2CAb2	102-150	305	235	460	54.1	51.7	80.4	174.2	99.63	7.39	0.30	10	6.24	0.41	0.24	11.14	8.93	17.82	100
Pedon 3, Representative soil located in downstream (greenschist parent rock), Fine loamy, Mixed, Superactive, mesic Typic Hapludalf																			
Oi	0-2	-	-	-	-	-	-	-	-	-	-	-	-	-	-	-	-	-	-
A	0-22	260	495	245	97	44.1	30.8	41.98	31.15	6.07	0.35	10	31.2	0.16	0.79	11.88	3.17	29.74	53.79
Bt1	22-61	345	440	215	76.1	48.9	27.7	38.85	23.43	5.18	0.20	6	13.9	0.16	0.34	7.42	4.76	25.11	50.51
Bt2	61-94	320	480	200	90.8	39.9	20.6	29	19.8	4.87	0.32	2	12.48	0.66	0.29	4.45	9.88	26.00	58.80
BCt	94-119	300	435	265	118	59.7	28.5	38.77	19.65	4.86	0.27	2	10.53	0.41	0.29	6.68	7.65	24.23	62.06
CBt	119-150	235	390	375	115	74.6	48.7	81.3	55.77	4.79	0.48	4	5.85	0.66	0.19	6.68	5.50	21.54	60.54
Pedon 4, Flooded soil located in downstream (greenschist parent rock), Sandy, Mixed, Superactive, mesic Typic Udifluvent																			
Oi	0-1	-	-	-	-	-	-	-	-	-	-	-	-	-	-	-	-	-	-
A	1-10	130	245	625	229	170	119	74.65	32.1	6.80	1.02	22	39.78	0.41	0.24	11.14	11.8	21.80	100
C1	10.26	10	135	855	216	211	291	86.45	50.67	7.46	0.52	46	2.34	0.24	0.14	11.88	1.74	2.27	100
C2	26-33	5	70	925	159	269	347	134.3	15.65	7.35	0.29	54	1.56	0.16	0.09	11.14	1.05	3.41	100
2C3	33-39	75	275	650	292	173	120	53.28	11.88	7.50	0.50	44	5.46	0.41	0.34	11.88	2.46	5.51	100
2C4	39-45	2.5	57.5	940	119	230	314	219.3	57.48	7.43	0.32	70	9.75	0.16	0.14	9.65	2.53	6.72	100
3C5	45-120	10	55	935	301	85.5	185	363.4	0.42	7.41	0.42	64	4.68	0.16	0.19	10.39	0.36	2.19	100

[1] VFS = very fine sand (0.05–0.10 mm), FS = fine sand (0.10– 0.25mm), MS = medium sand (0.25–0.50 mm); VC = coarse sand (0.50–1.00 mm), VCS = very coarse sand (1.00–2.00 mm); [2] pH in saturation paste; [3] EC= electrical conductivity in extract of soil; [4] OC= organic carbon; [5] CCE= calcium carbonate equivalent; [6] CEC= cation exchange capacity; [7] BS= base saturation

Table 3. Some micromorphological properties of horizons for the selected pedons

Horizon	Depth (cm)	Microstructure			Mineral component [d]	Organic component[e]	C/F Related Distribution[f]	B-Fabric [g]	C/F[h] (10μ)	Pedofeatures	MISECA (Degree of soil development)
		Aggregates[a]	Grade of pedality[b]	Voids [c]							
Pedon 1, Representative soil located in upstream (shale parent rock), Fine loamy, Mixed, Superactive, mesic Typic Dystrudept											
Oi	0-2	-	-	-	-	-	-	-	-	-	-
A	2-16	Gr, Cr	M, S	Vu, Cdp, Cdx, Chn, Chm	Qu, Kf, Op, Bi, Ch	Wo, Or, Lt, Gtr	Po	Ss, Msp, Gs, Un	40/60	Excrement, non-laminated hypo-coating of clay around void and rock, lithorelict of shale	8, weakly developed
BAt	16-34	Gr, Sb	M, W	Sp, vu, Chn, Chm	Qu, Kf, Op, Ch, Mu, Bi	Of, Pao	Po	Ss, Msp	40/60	Excrement, Fe/Mn oxide typic nodule, lithorelict of shale	7, weakly developed
Bt1	34-69	Sb	M	Vu, Chn, Chm	Qu, Kf, Ch, Op	Or, Lt	Po	Ss, Msp	30/70	Typic Fe/Mn oxide nodule, lithorelict of shale	8, weakly developed
Bt2	69-96	Sb	M, W	Chn, Pn, Vu	Qu, Op	Or, Pi	Po	Ss, Msp	55/45	Fe/Mn oxide concentric nodule with diffuse boundary, fragmented clay coatings, lithorelict of shale	10, moderately developed
C	96-150	-	W	Vu	Qu, Kf, Ch, Op	Or, Lt	Po	Ss, Un	70/30	lithorelict of shale, Geodic Fe/Mn oxide nodule	7, moderately developed
Pedon 2, Flooded soil located in upstream (shale parent rock), Fine loamy, Mixed, Superactive, mesic Typic Udifluvent											
Oi	0-1	-	-	-	-	-	-	-	-	-	
A	1-13	Gr, Cr	W	Vu, Pn	Qu, Kf, Ca, Op	Or, Gtr, Pi	Po	Ss, Cr, Un	70/30	Geodic Fe/Mn oxide nodule, Calcite nodule, flooded coating, charcoal	7, weakly developed
AC	13-51	Gr	M, W	Vu, Pn, Cdp	Qu, Ca, F, Mu, Ch, Op	Or, Lt	Po	Ss, Uns, Un	50/50	Typic Fe/Mn oxide rounded nodule, charcoal, lithorelict of shale, Excrements	6, weakly developed
C1	51-64	-	W	Vu	Qu, Ca, Op, Cpx	Or, Lt	Po	Un, Ss	50/50	Typic Fe/Mn oxide rounded nodule, charcoal, lithorelict of shale	7, weakly developed
C2	64-79	-	M, W	Vu	Qu, Ca, Bi, Ch, Mu, Kf, Op, Cpx	Or, Of, Lt	Po, Ch	Ss, Gs, Un	70/30	Calcitic hypo-coating, clay and silt hypo-coating	6, weakly developed
2CAb1	79-102	Gr	M	Vu, Cdp	Qu, Ca, Bi, Mu, Kf, Op, Cpx	Or, Lt, Pi	Po	Ss, Cr, Un	50/50	Infilling of calcite, lithorelict of shale	8, weakly developed
2CAb2	102-150	Sb	M	Vu, Chn, Chm	Qu, Bi, Ch, Mu, Kf, Op	Lt, Pi	Po	Un, Ss, Ms	60/40	lithorelict of shale, Typic Fe/Mn oxide rounded and unrounded nodule	10, moderately developed
Pedon 3, Representative soil located in downstream (greenschist parent rock), Fine loamy, Mixed, Superactive, mesic Typic Hapludalf											
Oi	0-2	-	-	-	-	-	-	-	-	-	-
A	2-22	Gr	M	Cdp, Chn, Chm,V	Qu, Kf, Ch	Gtr, Or	Po	Ss	45/55	Excrements	8, weakly developed
Bt1	22-61	Sb	M, W	Chn, Chm, Vu	Qu, Kf, Pl, Mu	Or, Pi	Po	Ss, Gs	60/40	Geodic Fe/Mn nodule, non-laminated hypo-coating of clay around void and rock	10, moderately developed
Bt2	61-94	Sb	M, W	Chn, Chm, Vu	Qu, Kf, Pl, Mu, Cpx	Or, Lt	Po, Ch	Ss, Msp	55/45	Micro-laminated coating of clay around void, Fe/Mn oxide coatings on void walls	13. moderately developed
BCt	94-119	Sb	W	Chn, Chm,Vu, Ve	Qu, Kf, Pl, Cpx	Or	Po, Ch	Ss, Pos	65/35	Micro-laminated coating of clay around void, Fe/Mn oxide coatings on void walls, Typic Fe/Mn nodule	10. moderately developed
CBt	119-150	Sb	W	Chn, Chm, Pn,Vu	Qu, Kf, Pl, Op, Cpx	-	Po, Ch	Ss, Msp, Uns	70/30	Fe/Mn oxide coatings on channel pore walls	11. moderately developed
Pedon 4, Flooded soil located in downstream (greenschist parent rock), Sandy, Mixed, Superactive, mesic Typic Udifluvent											
Oi	0-1	-	-	-	-	-	-	-	-	-	-
A	1-10	Gr	W	Vu, Cdp, Chn, Chm	Qu, Ca, Op, Cpx, Ch, Kf	Or, Lt	Po	Un, Ss	80/20	Rock fragment, hypo-coating of clay and silt, charcoal	5, weakly developed
C1	10.26	Sb	W	Chn, Chm, Vu	Qu, Ca, Op, Kf, Bi, Ch, Cpx	Of, Lt	Po, Ch	Ss, Cr, Uns	90/10	Typic Fe/Mn oxide nodule	5, weakly developed
C2	26-33	-	W	Vu	Qu , Ca, Op, Cpx, Ch, Mu, Ol	Lt, Pi	Po	Cr, Un	95/5	Typic Fe/Mn oxide nodule, Rock fragment	3, weakly developed
2C3	33-39	-	W	Chn, Chm, Vu	Qu, Kf, Ca, Cpx, Bi	Lt	Po	Ss, Cr, Un	50/50	Flooded coating, Rock fragment, Excrements	6, weakly developed
2C4	39-45	-	W	Vu	Kf, Qu, Mu, Cpx, Ca, Ch	Lt	Po	Cr, Un	90/10	Charcoal, Rock fragment	3, weakly developed
3C5	45-120	-	W	Vu	Qu, Kf, Op, Mu, Cpx, Ol	Lt	Po	Cr, Un	95/5	Charcoal, Rock fragment	3, weakly developed

[1] Gr- granule, Sb- subangular blockey, Cr- crumb; [2] S- strongly developed, M- moderately developed, W- weakly developed; [3]Vu- vagh, Cdp- compound packing, Cxp- complex packing, Chn- channel, Chm- chamber, Pn- planes; [4] Qu- quartz, Kf- K-feldespare, Op- opaques, Pl- plagioclase, Mu-muscovite, Cpx-clinopyroxene, Bi-biotite, Ch- chlorite, Ol- Olivine, Ca-calcite; [5]Tf- tissue fragments, Of- organ fragment, Or- organ residues, Pi- organic pigment, Gtr- general tissue residues, Lt- lignified tissues; [6]Ch- Chitonic, Po- Porphyric; [7] Ss- stipple speckled, Un- undifferentiated, Cr- crystallitic, Pos- poro-striated, Gs- grano-striated, Uns- unistrial; [8]C/F- the ratio between the part occupied by the coarse and fine material, respectively.

Mineral grains like biotite were found prone to weathering and resistant with large size in all soil layers. Bakhshandeh et al., (2014) reported alteration of biotite to chlorite which was common in north of Iran soils. Chlorites (commonly green colored) are associated with metamorphic rocks such as phyllite or greenschist appear by alteration products of biotite and other fero-magnesium minerals (Barnhisel & Bertsch, 1989). Angelucci (2006) with study of flooded terrace of the Guadiana River has reported that main part of mineral grains and rock fragments may derived from local bedrock or the reworking of pre-existing alluvial deposits. Presence of pyroxene (as large fragment in surface layers) and olivine was truly remarkable in flooded soils located in the downstream. Although some pyroxene was fresh, but others were subjected to strong weathering. Also, Owliaie et al., (2005) reported that feldspars, biotite, olivine and pyroxenes (primary Fe-bearing minerals) are extremely unstable in soils, eventually being transformed to secondary minerals. Certini et al., (2006) observed that weathering of pyroxenes in wetter climate (Mediterranean climate of central Italy) is showing iron oxides lining cleavage planes and fractures, as well as bleaching of the edges of crystals. Most altered rock fragments with strongly parallel oriented fine clay were observed in representative soils developed on greenschist parent rocks and probably formed by weathering of biotite grains. They may be confused with fragments clay coatings that contain of illuvial clay (Kuhn et al., 2010). In soils, muscovite often occurs as a replacement of weathered feldspars (Fitzpatrick, 1984). Ramezanpour & Pourmasoumi (2012) reported that some feldspars show slight to extreme hydrothermal alteration to sericite and clay neogenesis. All alteration products of muscovite were not recognized well. Likely, it can be changed to kaolinite (Fitzpatrick, 1984). The microscopic features of flooded soil in downstream (pedon 4) were slightly different from those observed in the other pedons. The difference was primarily related to coarse texture and heterogeneity.

Translocation of pedogenic carbonates as sparitic (macrocrystalline, >20μm) and micritic (microcrystalline, <4 μm) fragments were most noticeable in soil matrix and fragments of aggregate (pedorelicts) in both flooded soils, while various features of calcite did not exist in representative soils. The formation of pedogenic carbonates involves complex processes of precipitation, weathering (by dissolution) and translocation as mentioned by Khormali et al., (2006). Pedogenic calcite is recorded from a wide variety of soils, especially calcareous soils in arid areas; but, its presence in flooded soils can be related to translocation and then weathering of calcite in post-flooded soils. One of the main problems in studying the origins of carbonate minerals such as calcite in soil is deciding which primary minerals are formed through pedogenic process (secondary) and primary minerals remains from the original parent material. Distinguishing primary from secondary calcite may require a combination of evidence from field morphology and micromorphological investigation (Doner and Lynn, 1989).

In our study, various types of b-fabrics were recognized in representative and flooded soils. The b-fabric ranges from undifferentiated to crystallitic and unistrial depending on the composition of the material in flooded soils. Mallol (2006) observed the light brownish gray speckled groundmass with a weakly striated to unistrial b-fabrics in flooded sediments. Furthermore, calcitic crystallitic b-fabric was abundant in flooded soils. Brewer (1964) proposed terms of strial plasmic fabric (equivalent to the strial b-fabric) for description of the fabric of unconsolidated clayey sediments. In addition, Spaargaren et al., (1981) reported that unistrial b-fabrics are typical of undisturbed sediments in the lower horizons of soil profiles. Later, strial b-fabric sedimented or translocated material and transported soils were recognized by Mucher et al., (2010). Unistrial b-fabric which is related to sedimentation process of sedimentary rocks may be altered under pedogenic process to other b-fabrics such as speckled and striated with time.

In flooded soils, fragments of aggregate (pedorelicts) and rock fragments are extensively reworked by flow. Therefore, some soil layers contained rounded and non-rounded aggregates that have been eroded from another soil and composed from fine material. The fresh and weathered rock fragments were observed in flooded and representative soils.

Lithologic discontinuities provide important information about parent material origins (Schaetzl & Anderson, 2007). Both the morphological and micromorphological results showed lithologic discontinuities in both flooded soils. Marked differences in the size and shape of resistant minerals in some horizon are indicators of differences in materials (Soil Survey Staff. 2014) that occurred in flooded soil in downstream (2C4 and 3C5 horizons).

Since the soil moisture regime was Udic, the conditions were suitable for clay illuviation. Speckled b-fabric of the argillic horizon indicate that the forest land had high stability allowing the downward leaching of the upper horizons and subsequent clay movement (Khormali & Shamsi, 2009) that occurred in representative soils developed on greenschist parent rocks. There is no evidence of illuvial clay coating in flooded soils, but a kind of coatings which was called flood coatings by Brammer (1971) with clay-size fractions, silt and humus observed in flooded soils. However, the thickness of flood coatings formed on flooded soils was thin and it can be related to direct function of the clay and silt concentration of the suspension. Brammer (1971) reported that illuvial horizons formed in flooded soils cannot be classified as argillic because of lack of differential movement of fine clay and absence of strong orientation of translocated clay.

Study of the occurrence and distribution of iron oxides and their influence on soil properties as an important tool could help to understand pedogenetic processes of soils (Rezapour et al., 2010 and Alamdari et al., 2010). Redoximorphic features are common in most soils where water saturation occurs (Lindbo et al., 2010). There were many Fe/Mn oxides in the form of diffuse spots or stripes in flooded and representative soils. Despite the physical role of Fe/Mn oxides and calcite pedofeatures in pore formation (Gargiulo et al., 2013), Fe/Mn oxides in flooded soils were diffused in soil matrix such as amorphous discontinuous coating and have not any role in aggregation. Kirk (2004) reported that the surface intermittently flooded soils typically contains discontinuous coatings of amorphous iron oxides on other clay minerals, and under flooding, reduced iron is to a large extent re-precipitated as amorphous hydroxide.

Organic matter provides the food or substrate for soil microbes as well as fauna and have key influence on soil biological attribute (Rezaei et al., 2015). A wide range of organic matters such as poorly decomposed plant residues (with a recognizable cell structure) and decomposed organic matters (unrecognized structures) observed in flooded soils. They are sporadically occurred in soil layers and often had not any orientation. Mallol (2006) recorded the number of rootlets and scattered organ matter in sediments of flooded soils. Since the origin and initial degree of decomposition of the plant organs and remains in depositional environments such as floodplains may be unknown (Stolt & Lindbo, 2010). Therefore, identification of the pathways leading to decomposition of plant remains is difficult. On the other hand, there is not any idea about organic matter, which formed in situ (by plant cover after sedimentation) or transported with flow.

The presence of charcoal with translocational origin can be confirmed the evidence of forest fire in the study area. Annual forest fires in north of Iran is the main problem and induce changes in soil properties. They normally occur in autumn when forest floor litter dries due to hot-dry winds (Norouzi & Ramezanpour, 2013). The presence of charcoal and poorly sorted and unsorted mineral grains were relatively common in flooded soils, which confirm Fedoroff et al., (2010) report about preservation of charcoal fragments especially in buried soils. In addition, Charcoal could be the product of sporadic human activities that took place in the surroundings. The presence of artefacts in soil is generally a good indicator of human influence (Bullock et al., 1985) that presence of some man-made artefacts with strange shapes (mineral fragment) collected in flooded soils that may be related to some anthropogenic working. Anthropogenic activities such as agriculture, pegmatite and peridotite rocks mining and tourism have increased during these years in the watershed. These anthropogenic inputs probably are translocated during flooding sedimentation process which confirm the results reported by Mallol (2006).

5. CONCLUSION

The comparison of minerals in flooded and non-flooded (representative) soils indicated that origin of some materials in flooded soils were from susceptible and weatherable parent rocks. Moreover, the presence of calcite features and olivine mineral as angular and irregular shapes in different flooded soil layers confirm flooding in different times. The micromorphological results demonstrate differences in c/f related distribution pattern, b-fabric, microstructure and pedofeatures between flooded and representative soils. The MISECA values showed low grade evolution of the soil layers in flooded soils especially in downstream which had unconsolidated materials. Furthermore, these studies highlight the role of forest destruction as well as human activity on soil flooding in the Masoule Rudkhan watershed. It is often difficult to determine the origin of heterogeneous layers in flooded soils. However, it should be noted that additional techniques and further studies are needed for the identification of different sediments and soil materials in flooded lands.

Acknowledgement

We would like to express the gratitude towards university of Tabriz and faculty of agricultural sciences in the University of Guilan. The authors would like to thank the Natural Resources Organization of Guilan province for their valuable information on this study.

REFERENCES

Achyuthan, H., & Fedoroff, N. 2008. *Ferricretes in Tamil Nadu, Chennai, South-Eastern India: from landscape to micromorphology, genesis, and Paleoenvironmental Significance*, In: Kapur, S. Mermut, A. Stoops, G. (Eds.). New Trends in Soil Micromorphology, Springer-Verlag Berlin Heidelberg. pp. 111-136.

Alamdari, P., Jafarzadeh, A. A., Oustan, S., & Toomanian, N. 2010. *Iron oxide forms and distribution in a transect of Dasht-e-Tabriz soils, north-west Iran*. Journal of Food Agriculture and Environment. 8, 976-979.

Angelucci, D. E. 2006. *Micromorphological observations on some samples from the prehistoric site of Barca do Xerez de Baixo (Reguengos de Monsaraz, Portugal)*. Revista Portuguesa de Arqueologia, 9, 5-19.

Bakhshandeh, S., Norouzi, M., Heidari, S., & Bakhshandeh, S. 2014. *The role of parent material on soil properties in sloping areas under tea plantation in lahijan Iran*. Carpathian Journal of Earth and Environmental Sciences, 9, 159-170.

Barnhisel, R. I., & Bertsch, P. M. 1989. *Chlorites and hydroxyl-interlayered vermiculite and smectite*, In: Dixon, J.M. and Weed, S.B. (Eds.), Minerals in soil environments, Second Edition, Soil Sci. Soc. Am. Press, Madison, Wisconsin, USA. pp. 729-788.

Brammer, H. 1971. *Coatings in seasonally flooded soils*. Geoderma, 6, 5-16.

Brewer, R. 1964. *Fabric and Mineral Analysis of Soils*. John Wiley & Sons, Inc., New York.

Brewer, R. 1976. *Fabric and Mineral Analysis of Soils*. E. Krieger Pub. Co., Huntington, New York.

Bullock, P., Fedoroff, N., Jongerius, A., Stoops, G., & Tursina, T. 1985. *Handbook for thin section description.* Waine Res. Publ., Albrighton, England, 152 p.

Certini, G., Wilson, M. J., Hillier, S. J., Fraser, A. R. & Delbos, E. 2006. *Mineral weathering in trachydacitic derived soils and saprolites involving formation of embryonic halloysite and gibbsite at Mt. Amiata, Central Italy*. Geoderma, 133, 173–190.

Courty, M. A., Crisci, A., Fedoroff, M., Grice, K., Greenwood, P., Mermoux, M., Smith, D., & Thiemens, M. 2008. *Regional Manifestation of the Widespread Disruption of Soil-Landscapes by the 4 kyr BP Impact-Linked Dust Event Using Pedo-Sedimentary Micro-Fabrics*, In: Kapur, S. Mermut, A. Stoops, G. (Eds.). New Trends in Soil Micromorphology, Springer-Verlag Berlin Heidelberg. pp. 211-236.

Darvishzade, A., 2002. *Geology of Iran*. Amirkabir University of Technology Press. (In Persian).

Doner, H. E., & Lynn, W. C. 1989. *Carbonate, halide, sulfate and sulfide minerals*, In: Dixon, J.M. and Weed, S.B. (Eds.), Minerals in soil environments, Second Edition, Soil Sci. Soc. Am. Press, Madison, Wisconsin, USA. pp. 279-330.

Eze, P. N. Knight, J. & Evans, M. 2016. *Tracing recent environmental changes and pedogenesis using geochemistry and micromorphology of alluvial soils, Sabie-Sand River Basin, South Africa.* Geomorphology, 268, 312–321.

Fedoroff, N., Courty, M. A., & Guo, Z. 2010. *Palaeosoils and Relict Soils*. In: Stoops, G., Marcelino, V., Mees, F. (Eds.). Interpretation of micromorphological features of soils and regoliths. Elsevier B.V. UK. pp. 129-147.

Fitzpatrick, E. A. 1984. *Micromorphology of soils*. Chapman and Hall Ltd. NY. USA.

Gao, Z. Q. & Guan, X. M. 1994. *Micromorphological characteristics of soils of different fertility in north eastern China*, In: Ringrose-Voase, A.J. Humphreys, G.S. (Eds.). soil micromorphology: studies in management and genesis, Developments in Soil Science 22. Elsevier, Amsterdam, the Netherlands, pp. 651-658.

Gargiulo, L., Mele, G., & Terribile, F. 2013. *Image analysis and soil micromorphology applied to study physical mechanisms of soil pore development: An experiment using iron oxides and calcium carbonate*. Geoderma, 197–198, 151–160.

Gee, G. W. & Or, D. 2002. *Particle-size analysis.* In: Dane, J.H., Topp, G.C. (Eds.), Methods of soil analysis, Part 4- Physical methods. Agronomy Monograph, vol. 9. ASA and SSSA, Madison, WI, pp. 255-293.

Ghergherechi, S., Khormali, F., Mahmoodi, S., & Ayoubi, S. 2009. *Micromorphology of argillic horizon development in loess derived soils of humid and subhumid regions of Golestan Province, Iran*. Journal of Soil & Water Research, 40, 130-138. (In Persian)

Helmke, P. A. & Sparks D. L. 1996. *Lithium, Sodium, Potassium, Rubidium and Cesium.* In: Sparks, D. L., (Eds.), Methods of soil analysis, Part 3-chemical methods. Agronomy Monograph, vol. 9. ASA and SSSA, Madison, WI, pp. 551–574.

Kemp, R. A. 2013. *Paleosols and wind-blown sediments-soil micromorphology.* In: Elias, S.A. and Mock C. J. (Eds.), Encyclopedia of quaternary science, Second edition. Elsevier, B.V. USA. pp. 381-391.

Khormali, F., Abtahi, A., Mahmoodi, S., & Stoops, G. 2003. *Argillic horizon development in calcareous soils of arid and semiarid regions of southern Iran.* Catena, 53, 273–301.

Khormali, F., Abtahib, A., & Stoops, G. 2006. *Micromorphology of calcitic features in highly calcareous soils of Fars Province, Southern Iran.* Geoderma, 132, 31–46.

Khormali, F. & Shamsi, S. 2009. *Micromorphology and quality attributes of the loess derived soils affected by land use change: a case study in Ghapan watershed, northern Iran.* Journal Mountain Science, 6, 197–204.

Kirk, G. 2004. *The Biogeochemistry of Submerged Soils.* John Wiley & Sons Ltd, West Sussex, England.

Kuhn, P., Aguilar, J., & Miedema, R. 2010. *Textural pedofeatures and related horizons*. In: Stoops, G., Marcelino, V., Mees, F. (Eds.). Interpretation of micromorphological features of soils and regoliths. Elsevier B.V. UK. pp. 217-250.

Lindbo, D. L., Stolt, M. H., & Vepraskas, M.J. 2010. *Redoximorphic features.* In: Stoops, G., Marcelino, V., Mees, F. (Eds.). Interpretation of micromorphological features of soils and regoliths. Elsevier B.V. UK. pp. 129-147.

Loeppert, R. H., & Suarez, D. L. 2002. *Carbonate and gypsum.* In: Sparks, D. L., Page, A.L., Helmke, P.A., Loeppert, R.H., Soltanpour, P.N., Tabatabai, M.A., Johnston, C.T., Sumner, M.E. (Eds.), Methods of soil analysis, Part 3- chemical methods. Agronomy Monograph, vol. 9. ASA and SSSA, Madison, WI, pp. 575-601.

Mallol, C. 2006. *What's in a beach? Soil micromorphology of sediments from the Lower Paleolithic site of 'Ubeidiya, Israel.* Journal of Human Evolution, 51, 185-206.

Mucher, H., van Steijn, H. & Kwaad, F., 2010. *Colluvial and mass wasting deposits*. In: Stoops, G., Marcelino, V., Mees, F. (Eds.). Interpretation of micromorphological features of soils and regoliths. Elsevier B.V. UK. pp. 37–48.

Murphy, C. P. 1986. T*hin Section Preparation of Soils and Sediments*. A&B Academic Publ., Berkhamsted.

Nael, M., Khademi, H., Jalalian, A., Schulin, R., Kalbasi, M., & Sotohian, F. 2013**.** *Effect of geo-pedological conditions on the distribution and chemical speciation of selected trace elements in forest soils of western Alborz, Iran.* Geoderma, 152, 157–170.

Nelson, D. W., & Sommers, L. E. 1996. *Total carbone, organic carbone, and organic matter.* In: Sparks, D. L., Page, A.L., Helmke, P.A., Loeppert, R.H., Soltanpour, P.N., Tabatabai, M.A., Johnston, C.T., Sumner, M.E. (Eds.). Methods of soil analysis, Part 3- chemical methods. Agronomy Monograph, vol. 9. ASA and SSSA, Madison, WI, pp. 961-1010.

Norouzi, M., & Ramezanpour, H. 2013. *Effect of fire on soil nutrient availability in forests of Guilan, north of Iran*. Carpathian Journal of Earth and Environmental Sciences, 8(1), 157-170.

Owliaie, H.R., Heck, R.H., & Abtahi, A. 2005. *The magnetic susceptibility of soil in Kohgilouye, Iran.* Canadian Journal of Soil Science, 86, 97–107.

Ramezanpour, H., & Pourmasoumi, M. 2012. *Micromorphological aspects of two-forest soils development derived from igneous rocks in Lahijan, Iran.* Journal of Mountain Science, 9, 646–655.

Rezaei, H., Jafarzadeh, A. A., Aliasgharzad N., & Alipoor, L. 2015. *Soil quality investigation based on biological and micromorphological traits under different land uses.* Carpathian Journal of Earth and Environmental Sciences, 10, 241-254.

Rezapour, S., Golmohammad, H., & Ramezanpour, H. 2014. *Imapact of parent rock and topography aspect on the distribution of soil trace metals in natural ecosystems.* International Journal of Environmental Science and Technology, 11, 2075–2086.

Rezapour, S., Jafarzadeh, A. A., Samadi, A. & Oustan, S. 2010. *Distribution of iron oxides forms on a transect of calcareous soils, north-west of Iran.* Archives of Agronomy and Soil Science, 56, 165–182.

Rhoades, J.D. 1996. *Salinity: Electrical conductivityF and total dissolved solids.* In: Sparks, D. L., Page, A.L., Helmke, P.A., Loeppert, R.H., Soltanpour, P.N., Tabatabai, M.A., Johnston, C.T., Sumner, M.E. (Eds.). Methods of soil analysis, Part 3- chemical methods. Agronomy Monograph, vol. 9. ASA and SSSA, Madison, WI, pp. 417-435.

Schaetzl, R. J. & Anderson, S. 2007. *Soils, Genesis and Geomorphology.* Cambridge University Press.

Schoeneberger, P.J., Wysocki, D.A., Benham, E.C. & Soil Survey Staff. 2012. *Field book for describing and sampling soils.* Version 3.0. Natural Resources Conservation Service, National Soil Survey Center, Lincoln, NE.

Soil and water research institute. 1998. *Maps of soil moisture regimes.* Agriculture Research Organization, Ministry of Jihad-e-Agriculture. (In Persian)

Soil Survey Staff. 2014. *Keys to Soil Taxonomy.* 12th edition. United States Department of Agriculture & Natural Resources Conservation Service, Washington, DC.

Spaargaren, O. C., Creutzberg, D., van Reeuwijk, L. P. & van Diepen, C. A., 1981. *Thionic fluvisol (sulfic tropaquept). Central plain region, Thailand.* Soil Monolith Paper no. 1, International Soil Museum, Wageningen, the Netherlands.

Stolt, M.H., & Lindbo, D.L. 2010. *Soil Organic Matter.* In: Stoops, G., Marcelino, V., Mees, F. (Eds.). Interpretation of micromorphological features of soils and regoliths. Elsevier B.V. UK. pp. 369-396.

Stoops, G. 2003. *Guidelines for analysis and description of soil and regolith thin sections*, Soil Sci. Soc. Am., Inc. Madison, Wisconsin, USA.

Suarez, D.L. 1996. *Berylium, Magnesium, Calcium, Strontium, and Barium.* In: Sparks, D. L., Page, A.L., Helmke, P.A., Loeppert, R.H., Soltanpour, P.N., Tabatabai, M.A., Johnston, C.T., Sumner, M.E. (Eds.), Methods of soil analysis, Part 3- chemical methods. Agronomy Monograph, vol. 9. ASA and SSSA, Madison, WI, pp. 575-601.

Sumner, M. E., & Miller, W. P. 1996. *Cations exchange* *capacity and Exchange Coefficients.* In: Sparks, D. L., Page, A.L., Helmke, P.A., Loeppert, R.H., Soltanpour, P.N., Tabatabai, M.A., Johnston, C.T., Sumner, M.E. (Eds.). Methods of soil analysis, Part 3- chemical methods. Agronomy Monograph, vol. 9. ASA and SSSA, Madison, WI, pp. 1201-1230.

Teegavarapu, R. S. V. 2012. *Floods in a changing climate extreme precipitation*. Cambridge University Press. The Edinburgh Building, Cambridge, UK.

Thomas, G. W. 1996. *Soil pH and soil acidity*. In: Sparks, D. L., Page, A.L., Helmke, P.A., Loeppert, R.H., Soltanpour, P.N., Tabatabai, M.A., Johnston, C.T., Sumner, M.E. (Eds.). Methods of soil analysis, Part 3- chemical methods. Agronomy Monograph, vol. 9. ASA and SSSA, Madison, WI, pp. 475-490.

USDA 2017. *Soil survey manual*, Soil Science Division Staff, Handbook No. 18.

Yardley, B.W.D., MacKenzie, W.S., & Guilford, C. 1990. *Atlas of metamorphic rocks and their textures.* John Wiley & Sons, Inc., New York.

Zauyah, S., Schaefer, C. E. G. R., & Simas, F.N.B. 2010. *Saprolites.* In: Stoops, G., Marcelino, V., Mees, F. (Eds.). Interpretation of micromorphological features of soils and regoliths. Elsevier B.V. UK. pp. 49-68.

Zhuang, Y., Bao, W., & French, C. 2013. *River floodplain aggradation history and cultural activities: geoarchaeological investigation at the Yuezhuang site, Lower Yellow River, China*, Quaternary International, 315, 101-115.

Received at: 13. 09. 2017
Revised at: 31. 10. 2017
Accepted for publication at: 21. 12. 2017
Published online at: 28. 12. 2017